Stopped-flow Kinetic Studies of Cu^{2+} Ion Binding to Bovine Serum Albumin

Naohisa KURE, Hitoshi NAKATSUJI, Takayuki SANO, and Tatsuya YASUNAGA*
Faculty of Science, Hiroshima University, Higashisenda-machi, Naka-ku, Hiroshima 730
(Received March 17, 1984)

The interaction of Cu^{2+} ion with bovine serum albumin (BSA) was studied statically by equilibrium dialysis and ultraviolet spectrophotometric titration techniques, and kinetically by the stopped-flow method with transmittance detection at 255 nm. The static measurements showed the presence of one primary binding site and a number of weaker binding sites at pH 5.2. Stopped-flow measurements were undertaken in the pH region of 4—6.4 where a single reaction process was observed on the order of several seconds following the rapid absorbance change within the dead-time of the apparatus. This single reaction process was attributed to reaction of Cu^{2+} ion with the primary BSA site. The analyses of pH and concentration dependences of both the relaxation time and absorbance change confirmed the presence of two types of bound Cu^{2+} species to the primary binding site. One type formed during the dead-time of the apparatus is postulated as a square-planar complex formed between Cu^{2+} and the three N-terminal peptides of BSA. This reaction occurs with Cu^{2+} being exchanged for hydrogen ions on the N-terminal peptides. The second type of bound Cu^{2+}, observed by stopped-flow method is thought to result from a bimolecular binding of Cu^{2+} ion a deprotonated imidazolyl group in the third position of the histidyl residue; the value of the molar extinction coefficient for this species, determined kinetically, suggests a further coordination of the β-carboxyl group to the bound Cu^{2+}.

Various studies on the binding of Cu^{2+} ions to bovine serum albumin (BSA),[1-3] the 1—24 N-terminal peptide unit of BSA,[4-6] and the 1—4 N-terminal peptide unit of BSA[5] have confirmed the presence of at least two types of bound species in neutral and low pH regions. A chelated complex, predominant above pH 6, between Cu^{2+} ion and the three N-terminal peptides (Asp-Thr-His-) of BSA shows a square-planar configuration made by coordinations by α-amino, imidazolyl, and two peptide nitrogen atoms to the central Cu^{2+} ion.[3,4] Another type of species has been identified in the low pH range below 5.5. Iyer *et al.*[7] have reported the presence of two types of complexes between Cu^{2+} and N-terminal site of a synthetic peptide of human serum albumin (HSA) and have pointed out the necessity of kinetic studies for elucidation of the mechanism in forming of these complexes.

In the present study, the binding nature of Cu^{2+} ion to BSA was investigated both statically by equilibrium dialysis and ultraviolet (UV) spectrophotometric titration techniques and kinetically by stopped-flow measurements in the pH range where the two types of bound Cu^{2+} species coexist. A plausible mechanism of Cu^{2+} binding to the peptide sites is proposed; the molecular structure of the complexes is also discussed.

Experimental

Materials. Bovine serum albumin (prepared from Fraction V and essentially fatty acid-free) was purchased from Sigma Chem. Co. and used without further purification. The concentration of BSA was determined spectrophotometrically.[8] Solutions of Cu^{2+} ion were made by direct weighing of $CuSO_4$ anhydrous. The pH values of the solutions were adjusted by H_2SO_4 and/or KOH. No pH buffers were added. All measurements were made in 1 mM† solutions of K_2SO_4. Analytical grade reagents were used throughout.

Equilibrium Dialysis. The extent of binding was measured by the equilibrium dialysis technique at pH 5.2 with a dialysis cell (Sanko Plastics Co. type 5044-05) having ten separate chambers. After 72 to 84 hours of dialysis at 25±1 °C, concentrations of Cu^{2+} in the dialysed solutions were determined with a Perkin-Elmer Model 5000 atomic absorption spectrophotometer. The detection limit of this method for Cu^{2+} concentration was 1.5×10^{-7} M. The pH values of the dialysed solutions were 5.2±0.08.

Spectrophotometry. The difference spectra of BSA solutions in the presence and absence of Cu^{2+} ions were measured in the ultraviolet region using a Union Giken SM 401 spectrophotometer at 25±0.2 °C.

Stopped-flow Experiments. The kinetic measurements were carried out using a Union Giken Stopped-flow spectrophotometer RA 401. The dead-time of this apparatus is 5 ms. For the case of very small amplitudes, an accurate relaxation time was obtained by signal averaging 2—10 measurements using the averaging capabilities of the wave memory apparatus. All kinetic measurements were made at 25±0.2 °C.

Results and Discussion

Binding Parameters. Klotz and Curne[9] reported that at most there are sixteen sites on BSA for binding Cu^{2+} ions at pH 4.83, but data obtained in their study were limited to high binding conditions, *i.e.*, at a binding ratio, r, (moles of bound Cu^{2+}/moles of protein) >1.5. Naik *et al.*[10] determined the binding isotherm of Cu^{2+} with BSA at low binding conditions with the Cu^{2+} titration technique using a Cu^{2+} ion-specific electrode. However, in our investigations using the Cu^{2+} ion-specific electrode, we found that BSA ions significantly lower the voltage of the Cu^{2+} ion-specific electrode which results in serious errors in the binding data. Consequently, the binding data were obtained at low binding conditions using an equilibrium dialysis technique, measuring Cu^{2+} in dialysed solutions with atomic absorption.

Figure 1 illustrates a Scatchard plot of the binding of Cu^{2+} ion to BSA at pH 5.2±0.08. The shape of the isotherm reveals the existence of at least two classes of binding sites. The analysis of this plot, using the maximum number of Cu^{2+} sites per BSA molecule of 16,[9] yields the binding parameters: n_p=0.8—1.3, K_p=(5.5—8.8)$\times10^5$ M^{-1}, n_s=14.7—15.2, K_s=(5.4—5.8)×

† 1 M=1 mol dm^{-3}.

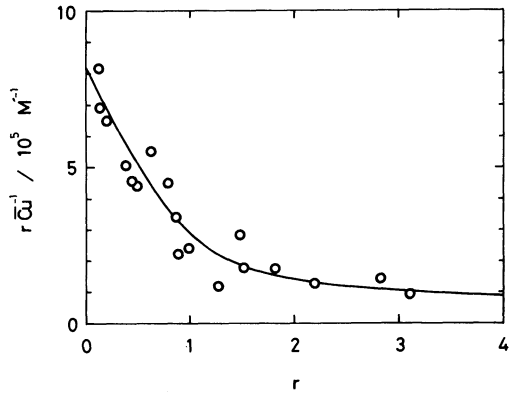

Fig. 1. Scatchard plot of the binding of Cu^{2+} ion to BSA in 1 mM K_2SO_4 solution at pH 5.2±0.08 and 25±1 °C. The circle represents the observed data, and the solid line shows the theoretical curve calculated using n_p=1, K_p=7.2×10^5 M^{-1}, n_s=15 and K_s= 5.6×10^3 M^{-1}.

10^3 M^{-1} where the n and K are the number of binding sites and the binding constants, respectively; the subscripts p and s refer to the primary and secondary binding sites, respectively. As can be seen in Fig. 1, the observed data fall on the theoretical curve calculated using these values. These results are consistent with the assignment of one primary binding site and fifteen secondary ones to the BSA molecule under the present pH conditions.

Ultraviolet Spectrophotometric Titration. The Cu^{2+}-BSA complex exhibits a strong ultraviolet (UV) absorption maximum around 250 mn in addition to two maxima at 525 nm and 650—700 nm in the visible region.[3,4] The absorption band around 250 nm, characteristic of Cu^{2+} complexes with amino acids[11,12] and peptides,[12-17] has been assigned to a charge transfer transition from amino, carboxylato, imidazolyl groups and ionized peptide nitrogen to Cu^{2+} ions. The absorbance increased linearly for this charge transfer absorption band up to a metal to protein ratio (M/P) of about unity at pH 5.2±0.02 as shown in Fig. 2(a). Since the absorbance of free Cu^{2+} ion is negligibly small at the present wavelength, the observed change in absorbance (ΔA^{255}) may be written as

$$\Delta A^{255}/\text{cm} = (\varepsilon^{255}_{c,app} - \varepsilon^{255}_{BSA}) \cdot \bar{C}, \quad (1)$$

where and ε^{255}_{BSA}, $\varepsilon^{255}_{c,app}$ and $\bar{C}$ denote the molar extinction coefficient of BSA, the apparent molar extinction coefficient of Cu^{2+}-BSA complex and its equilibrium concentration, respectively; the superscript 255 refers to the wavelength. The variation of $\varepsilon^{255}_{c,app}-\varepsilon^{255}_{BSA}$, which is given by calculating $\Delta A^{255}/\bar{C}$ using the binding parameters obtained above, was represented as a function of binding ratio r in Fig. 2 (b). Reasonable constancy of $\varepsilon^{255}_{c,app}-\varepsilon^{255}_{BSA}$ up to an r value of unity further confirms the presence of one primary binding site. The molar extinction coefficient $\varepsilon^{255}_{c,app}$ of the complex formed on the primary site was estimated to be 24500 $M^{-1}cm^{-1}$ by using a value of 21400 $M^{-1}cm^{-1}$ for ε^{255}_{BSA}.

Experimental Results in Stopped-flow Measurements. In order to elucidate the dynamic mechanism of the complex formation on the primary site, stopped-flow measurements were undertaken at a fixed and small

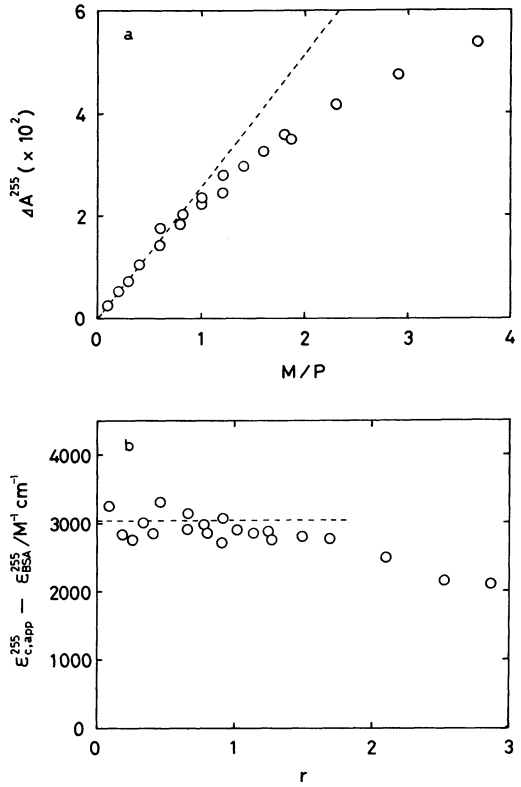

Fig. 2. (a) M/P dependence of the absorbance change (per 1 cm path-length) at 255 nm measured by titrating BSA (1.0×10^{-5} M) solutions with various amounts of Cu^{2+} ions, at pH 5.2±0.02 and 25± 0.2 °C. (b) A plot of $\varepsilon^{255}_{c,app}-\varepsilon^{255}_{BSA}$ *vs.* binding ratio r.

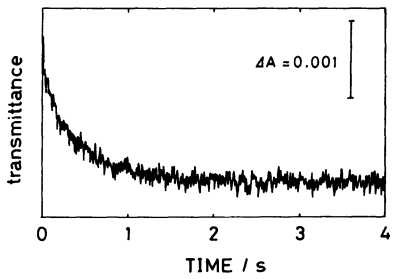

Fig. 3. A typical oscillographic trace of the stopped-flow experiment of the reaction between Cu^{2+} ion (2.0×10^{-6} M) and BSA (1.0×10^{-5} M) monitored by the change in the transmittance intensity (increasing upward) at 255 nm, pH 4.6 and 25±0.2 °C in 1 mM K_2SO_4 solution. The magnitude of the absorbance change is indicated by the bar in the upper right-hand corner.

M/P ratio of 0.2. The reaction between Cu^{2+} ion and BSA was followed by monitoring the change in transmittance at 255 nm. As shown in Fig. 3, a definite decrease in transmittance intensity was observed within several seconds at every pH value and concentration examined. Other reactions were not discernible within the time resolution of the apparatus (5 ms—100 s). The spectra of the solutions after mixing were quite stable over a period of two days.

The relaxation time of the reaction was determined by the semilogarithmic plot of the reaction curve near the equilibrium point. The variation of the reciprocal relaxation time (τ^{-1}) with pH, and with concentration

at pH 4.6 and 5.2 are represented in Figs. 4, 5, and 6, respectively.

The absorbance change (ΔA^{255}_{SF}) estimated from the reaction trace observed by the stopped-flow measurements, the total absorbance change (ΔA^{255}_{total}) due to reaction measured statically with a spectrophotometer at 255 nm, and the difference between ΔA^{255}_{total} and ΔA^{255}_{SF}, which corresponds to the absorbance change (ΔA^{255}_{DT}) within the dead-time of the stopped-flow apparatus are represented in Fig. 7 as a function of pH.

pH Dependence of Absorbance Changes. As can be seen in Fig. 7, the changes in the magnitude of ΔA^{255}_{SF} and ΔA^{255}_{total} as a function of pH reveal the presence of at least one rapid reaction process within the dead-time of the apparatus in addition to the one actually observed (see, *e.g.*, the change in ΔA^{255}_{DT}). The pH dependence of ΔA^{255}_{DT} implies that this rapid reaction involves the exchange of Cu^{2+} ions with hydrogen ions bound to BSA and that the complex formed from this process predominates above pH 6. These observed properties are characteristic of chelation complex formation between Cu^{2+} and the N-terminal three peptides (Asp-Thr-His-) of BSA, as has been reported in various studies on the binding of Cu^{2+} ions to BSA[3,4] and the model peptides of BSA.[4-6] Accordingly, the absorbance change within the dead-time is attributed to the formation of the chelation complex. On the other hand, ΔA^{255}_{SF} shows a quite different pH dependence, exhibiting a maximum around pH 4.8. This reveals that the reaction observed by the stopped-flow measurements results in a different kind of bound species from the chelated one. The bound species may correspond to the type of complex observed at low pH region in visible spectroscopic studies by others.[3,4]

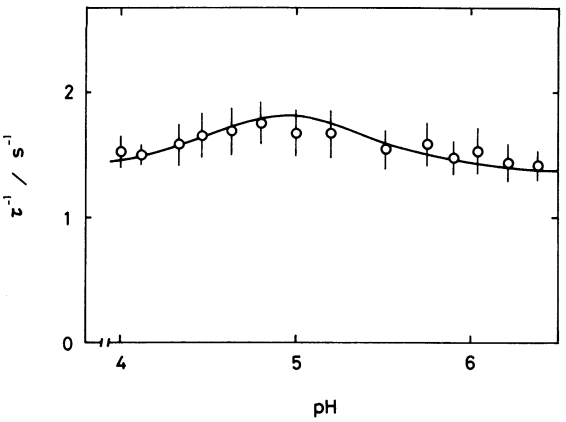

Fig. 4. The pH dependence of τ^{-1} at the fixed concentrations of Cu^{2+} ion (2.0×10^{-6} M) and BSA (1.0×10^{-5} M).

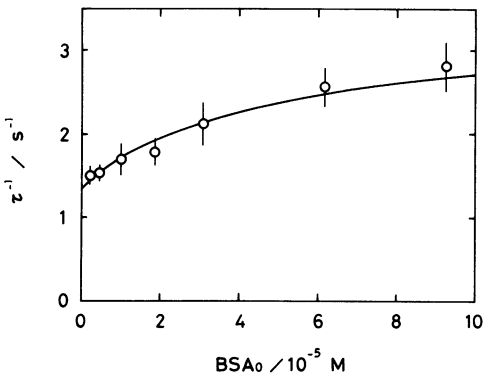

Fig. 5. The variation of τ^{-1} with the total concentration of BSA (BSA_0) at a fixed M/P of 0.2 and pH 4.6.

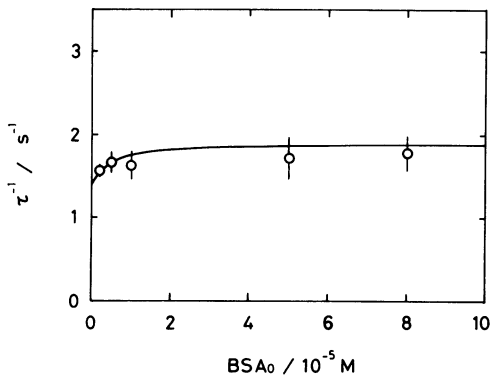

Fig. 6. The variation of τ^{-1} with the total concentration of BSA (BSA_0) at a fixed M/P of 0.2 and pH 5.2.

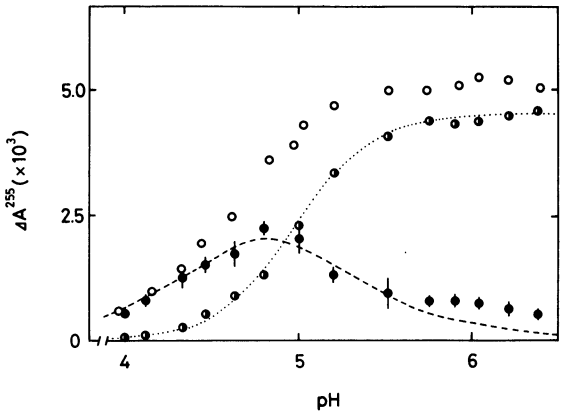

Fig. 7. The pH dependence of absorbance changes at 255 nm due to the reaction between Cu^{2+} (2.0×10^{-6} M) and BSA (1.0×10^{-5} M): ○, the total absorbance change (ΔA^{255}_{total}) measured spectrophotometrically; ●, the absorbance change (ΔA^{255}_{SF}) observed by stopped-flow method; ◑, the absorbance change within the dead-time of the stopped-flow apparatus (ΔA^{255}_{DT}) determined from $\Delta A^{255}_{total} - \Delta A^{255}_{SF}$ at each pH value.

Rapid Reaction within Dead-time of Apparatus. A reaction scheme of the chelation complex, formed rapidly within the dead-time of the apparatus, was examined on the basis of the pH dependence of ΔA^{255}_{DT}. In the neutral pH region, the three N-terminal peptides (Asp-Thr-His-) have three titratable hydrogen ions from the β-carboxyl and α-amino groups in the first terminal aspartly residue and from the imidazolyl group in the third possition of histidly residue. The pK_a values of these function groups, obtained from a titration study of the N-terminal 1—4 peptide of BSA by Bradshow *et al.*,[6] were 3.4, 7.7, and 6.7, respectively. As judged from these values, only the two deprotonation equilibria of the β-carboxyl and imidazolyl groups are important under the present pH range of 4—6.4. Therefore, the three N-terminal peptides of BSA may be represented by the following equilibria,

$$S_1 \underset{H}{\overset{K_{\beta c}}{\rightleftharpoons}} S_2 \underset{H}{\overset{K_{im}}{\rightleftharpoons}} S_3 \qquad \text{(I)}$$

H, $K_{\beta c}$, and K_{im} are the hydrogen ion and the deprotonation constants of β-carboxyl and imidazolyl groups, respectively; the S_i (i=1, 2, and 3) refer to the possible protonation and/or deprotonation states of the titratable groups on the three N-terminal peptides, defined as

S_1: Asp(protonated β-carboxyl)-Thr-His(protonated imidazolyl);

S_2: Asp(deprotonated β-carboxyl)-Thr-His(protonated imidazolyl);

S_3: Asp(deprotonated β-carboxyl)-Thr-His(deprotonated imidazolyl),

where α-amino group in the terminal aspartyl residue is protonated in every states. Since it is common for a transition metal ion to bind to a ligand in the protonated state by exchanging itself with a hydrogen ion,[18-20] every S_1, S_2, and S_3 are assumed to be available in the binding of Cu^{2+} ion. Under this assumption, by considering the competition of Cu^{2+} ion with the variously available hydrogen ions, the following reaction scheme was examined:

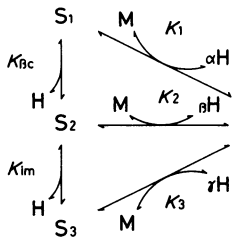

(II)

where M, C_a, and K_i (i= 1, 2, and 3) denote the free Cu^{2+} ion, the chelated complex and the binding constant of each step, respectively; and where α, β, and γ are the number of hydrogen ions released from each binding reaction step, respectively. The cyclic nature of the reaction requires

$$K_1 = K_{\beta c}K_2 = K_{\beta c}K_{im}K_3, \qquad (2)$$

$$\alpha = \beta + 1 = \gamma + 2. \qquad (3)$$

By use of the molar extinction coefficient ($\varepsilon^{255}_{C_a}$) of C_a and that of BSA, the equation of a net absorbance change resulting from the formation of C_a is given by

$$\Delta A^{255}_{DT}/\text{cm} = (\varepsilon^{255}_{C_a} - \varepsilon^{255}_{BSA}) \cdot \bar{C}_{a,r}, \qquad (4)$$

with

$$\bar{C}_{a,r} = \frac{1}{2A}\{A(M_0+S_0) + B - \sqrt{A^2(M_0-S_0)+2AB(M_0+S_0)+B^2}\}, \qquad (5)$$

$$A = K_1/\bar{H}_r^3, \qquad (6)$$

$$B = 1 + K_{\beta c}/\bar{H}_r + K_{\beta c}K_{im}/\bar{H}_r^2, \qquad (7)$$

where a bar with a subscript r and a subscript 0 refer to the equilibrium concentration after the rapid equilibria and the total concentration of each species, respectively. In the present analyses, the values of 4×10^{-4} M for $K_{\beta c}$ and 2×10^{-7} for K_{im} reported by Bradshow *et al.*,[6] were adopted. The equilibrium hydrogen ion concentration was approximated by the final concentration of hydrogen ion since the pH changes in solution after mixing were within ±0.03 of the initial pH. The observed ΔA^{255}_{DT}, plotted *vs.* $\bar{C}_{a,r}$ calculated for various values of α and K_1, is shown in Fig. 8. As can be seen in the figure, an excellent linear correlation passing through the origin was found for α=3 demonstrating the plausibility of reaction Scheme II. The values of K_1, K_2, and K_3 obtained using α=3 are listed in Table 1. From the slope of the straight line in Fig. 8, the value of $\varepsilon^{255}_{C_a}$ was estimated to be 23700 $M^{-1}cm^{-1}$. As can be seen in Fig. 7, the data of ΔA^{255}_{DT} fall on the theoretical curve (dotted line) calculated from Eqs. 4—7 using this value.

Reaction Process Observed by Stopped-flow Method. Since the reaction was observed under the conditions where complex formation at the primary site predominates, the following three types of reactions at the N-terminal site were considered: (a) Reactions succeeding the rapid formation of the chelation complex, (b) intermediate reactions occurring during the formation of chelation complex, and (c) reactions

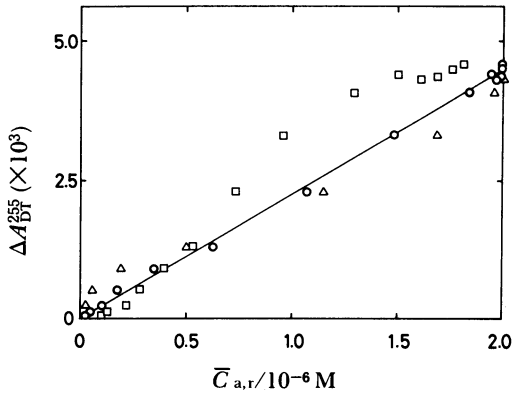

Fig. 8. Plots of ΔA^{255}_{DT} *vs.* $\bar{C}_{a,r}$ calculated for various values of α and K_1: □, α=2 and $K_1=2.4\times10^{-4}$ M; ○, α=3 and $K_1=4.8\times10^{-9}$ M^2; △, α=4 and $K_1=5.6\times10^{-14}$ M^3.

Table 1. Equilibrium and rate constants for binding of Cu^{2+} ion to BSA at 25°C and molar extinction coefficients of complexes at 255 nm

K_p[a]	K_1	K_2	K_3	K_b	k_b	k_{-b}	K_{app}[b]
10^5 M^{-1}	10^{-9} M^2	10^{-5} M		10^6 M^{-1}	10^6 $M^{-1}s^{-1}$	s^{-1}	10^5 M^{-1}
7.2±1.6	4.8±0.8	1.2±0.2	60±10	3.9±0.8	5.2±1.3	1.3±0.1	4.1±0.7

$\varepsilon^{255}_{c,app}$[a]	$\varepsilon^{255}_{C_a}$	$\varepsilon^{255}_{C_b}$	$\varepsilon^{255}_{c,app}$[b]
$M^{-1}cm^{-1}$	$M^{-1}cm^{-1}$	$M^{-1}cm^{-1}$	$M^{-1}cm^{-1}$
24500	23700	26200	24400

a) Statically obtained for the primary binding site at pH 5.2. b) Calculated from Eqs. 12 and 13 for pH 5.2 using equilibrium constants and molar extinction coefficients obtained kinetically.

essentially independent of the formation of the chelation complex. Among these, reactions in group (a) expected only at higher pH, were eliminated from consideration. Furthermore, since the present reaction takes place after the establishment of the chelation complex, reaction in group (b) could also be excluded. Therefore, only reactions in group (c) needed further investigation. As can be seen in Figs. 5 and 6, the difference in the concentration dependences of τ^{-1} obtained at different pH values implies the contribution of a specific protonation/deprotonation state of the N-terminal peptides to the present reaction, and the increase of τ^{-1} at pH 4.6 with increasing concentration suggests a bimolecular reaction. In addition, the approximate constancy in τ^{-1} obtained at various pH values as shown in Fig. 4 implies that hydrogen ions do not participate directly in the present reaction. These observations suggest a simple binding reaction of Cu^{2+} ion with the N-terminal peptides at a given pH-dependent state. Thus, bimolecular binding mechanisms between Cu^{2+} ion and the N-terminal site in each of three different states, designated with S_1, S_2, and S_3, were examined in detail. Among these, binding reactions with S_1 and S_2 were discounted due to poor agreement between the data and theoretical τ^{-1} calculated at the corresponding pH and concentration conditions. Subsequently, the binding reaction between Cu^{2+} ion and S_3 was examined. By combining the rapid equilibria (Scheme II) with the binding reaction, the mechanism is rewritten as

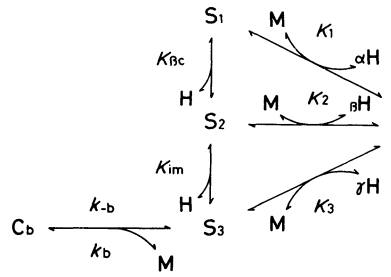

(III)

(present reaction) (rapid equilibria)

with

$$K_b = k_b/k_{-b}, \tag{8}$$

where k_b, k_{-b}, and K_b are the forward and backward rate constants and the equilibrium constant, respectively. Under the conditions of constant hydrogen ion concentration, the equation of τ^{-1} for the present reaction is given by

$$\tau^{-1} = k_{-b}\left[K_b\frac{\bar{S}_3(F-K_3\bar{M}/\bar{H})}{F(1+K_3\bar{S}_3/\bar{H})}+\frac{\bar{M}}{F}+1\right], \tag{9}$$

with

$$F = (1+\bar{H}/K_{\beta c})(\bar{H}+K_3\bar{S}_3)/K_{1m}+K_3(\bar{M}+\bar{S}_3)/\bar{H}+1, \tag{10}$$

where the overbar refers to the equilibrium concentration of each reacting species. The concentration term in the bracket in Eq. 9 was calculated for various values of K_b. A plot of τ^{-1} measured at various pH values and concentrations *vs.* the concentration term obtained for $K_b=3.9\times10^6\,M^{-1}$ gave a good correlation passing through the origin. From the slope of this line, the value of k_{-b} was determined to be $1.3\,s^{-1}$ and that of k_b calculated to be $5.2\times10^6\,M^{-1}s^{-1}$. Theoretical

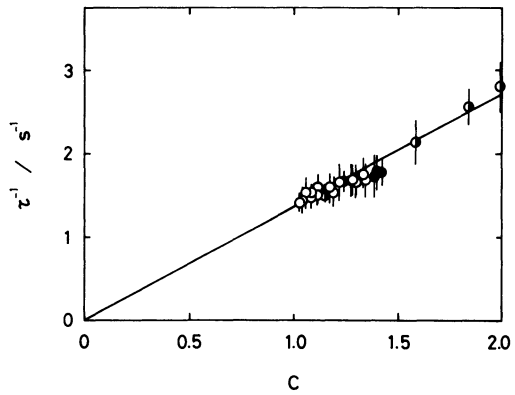

Fig. 9. A plot of τ^{-1} obtained at each pH value and concentration *vs.* the concentration term in Eq. 9, designated by C in this figure and calculated for $K_b=3.9\times10^6\,M^{-1}$.

curves of τ^{-1} obtained for these values are drawn in Figs. 4, 5, and 6, respectively. Good agreement between the theoretical curves and the data as shown in the figures confirms the plausibility of reaction mechanism III.

The absorbance change ΔA^{255}_{SF}, accompanying the present reaction is related linearly to the equilibrium concentration of the complexes as follows:

$$\Delta A^{255}_{SF}/cm = (\varepsilon^{255}_{C_a}-\varepsilon^{255}_{BSA})(\bar{C}_a-\bar{C}_{a,r}) + (\varepsilon^{255}_{C_b}-\varepsilon^{255}_{BSA})\bar{C}_b, \tag{11}$$

where $\varepsilon^{255}_{C_b}$ denotes the molar extinction coefficient of the complex C_b. As shown in Fig. 7, the variation of ΔA^{255}_{SF} with pH (drawn with the dashed line), calculated from Eq. 9 by use of the K_b value obtained above, for $\varepsilon^{255}_{C_b}=26200\ M^{-1}cm^{-1}$ gives good fit with data at each pH value. This fact further supports the validity of mechanism III.

The equilibrium and rate constants and the molar extinction coefficients (at 255 nm) of the complexes determined in the present analyses are summarized in Table 1. Using these values, the apparent association constant K_{app}, defined as $(\bar{C}_a+\bar{C}_b)/(\bar{S}_1+\bar{S}_2+\bar{S}_3)\cdot\bar{M}$, and the apparent molar extinction coefficient $\varepsilon^{255}_{c,app}$, can be calculated from the following relations:

$$K_{app} = \frac{K_1/\bar{H}+K_{\beta c}K_{1m}K_b/\bar{H}^2}{1+K_{\beta c}/\bar{H}+K_{\beta c}K_{1m}/\bar{H}^2}, \tag{12}$$

and

$$\varepsilon^{255}_{c,app} = \frac{\varepsilon^{255}_{C_a}\bar{C}_a+\varepsilon^{255}_{C_b}\bar{C}_b}{\bar{C}_a+\bar{C}_b}. \tag{13}$$

The values calculated for pH 5.2 are also listed in Table 1 together with those of K_p and $\varepsilon^{255}_{c,app}$ obtained from the equilibrium dialysis and UV spectrophotometric titration studies performed at pH 5.2, for the primary complex on BSA. The agreement between the values obtained kinetically and statically strongly support mechanism III as well as the assumptions adopted.

The presence of a Cu^{2+}–BSA complex at low pH, appearing below pH 5.5 and exhibiting a broad maximum around 650—700 nm, was confirmed by Breslow,[3] and Peters and Blumenstock.[4] However, the specific binding site on BSA of this complex has not yet been clarified. The present static and kinetic studies reveal that the low pH complex, detected directly by stopped-flow method, is formed in competition with

the chelation complex on the N-terminal site of BSA. This consists with the results of the potentiometric titration study[7] of the binding between Cu^{2+} and a derivative of the native-sequence tripeptide (Asp-Ala-His-NHMe)[21] of the N-terminal site of human serum albumin (HSA). Some useful information regarding the structure of the low pH complex can be derived from the present kinetic results. As shown in Scheme III, the selective formation of the low pH complex in the specific state, S_3, reveals the coordination of a deprotonated nitrogen atom of imidazolyl group with the Cu^{2+} ion. Furthermore, the absence of the proton release in this process supports further the suggestion, by Breslow based on the visible spectroscopy,[3] that the coordination of peptide nitrogen atoms may not be involved in the structure of low pH complex. In addition, the larger value in the molar extinction coefficient of the low pH complex ($\varepsilon_{C_b}^{255}=26200$) compared to that of chelated one ($\varepsilon_{C_a}^{255}=23700$) suggests a charge transfer from the oxygen atom rather than nitrogen atom; hence, the low pH complex likely involves the β-carboxylato group of the terminal aspartyl residue. From these observations, the most likely configuration for the low pH complex is a *di*-coordinated structure involving a nitrogen atom of imidazolyl group and an oxygen atom of β-carboxylato group. The rate-determining step for the coordination of the small ligands to Cu^{2+} ion has been assigned to the metal-water exchange process (10^7—10^9 $M^{-1}s^{-1}$).[22-26] However, the value of 5.2×10^6 $M^{-1}s^{-1}$ for the second-order formation rate constant k_b is small compared to those values. This implies a higher activation energy is involved in the formation process of the low pH Cu^{2+}-BSA complex. One possible explanation is that a conformational change is the rate-determining process which is required to allow the β-carboxylato group to coordinate to the bound Cu^{2+}.

On the other hand, the chelation complex is formed faster than the time resolution of the present stopped-flow apparatus. As shown by Scheme III and the pK_a values of each N-terminal site group, at most two hydrogen ions are expelled by the formation of the chelation complex in the range of pH 5—6. In contrast with the present result, the square-planar structure of the chelation complex, originally proposed by Peters and Blumenstock[4] and further supported by Shearer *et al.*,[5] requires four released hydrogen ions in the corresponding pH region. This inconsistency in the number of released hydrogen ions may imply that only two hydrogen ions of the four possible compete with Cu^{2+} ion in the formation of the chelation complex. Further elucidation requires application of a rapid relaxation technique to the present system.

References

1) I. M. Kolthoff and B. R. Willeford, *J. Am. Chem. Soc.*, **80**, 5673 (1958).
2) T. Peters, Jr., *Biochim. Biophys. Acta*, **39**, 546 (1960).
3) E. Breslow, *J. Biol. Chem.*, **239**, 3252 (1964).
4) T. Peters and F. A. Blumenstock, *J. Biol. Chem.*, **242**, 1574 (1967).
5) W. T. Shearer, R. A. Bradshow, and F. R. N. Gurd, *J. Biol. Chem.*, **242**, 5451 (1967).
6) R. A. Bradshow, W. T. Shearer, and F. R. N. Gurd, *J. Biol. Chem.*, **243**, 3817 (1968).
7) K. S. Iyer, S. Lau, S. H. Laurie, and B. Sarker, *Biochem. J.*, **169**, 61 (1978).
8) E. J. Cohn, W. L. Hubhes, and J. H. Weare, *J. Am. Chem. Soc.*, **69**, 1753 (1947).
9) I. M. Klotz and H. G. Curme, *J. Am. Chem. Soc.*, **70**, 939 (1946).
10) D. V. Naik, C. F. Jewell, and S. G. Schulman, *J. Pharm. Sci.*, **64**, 1243 (1975).
11) D. W. Urry and H. Eyring, *J. Am. Chem. Soc.*, **86**, 4574 (1964).
12) J. M. Tsangaris, J. W. Chang, and R. B. Martin, *J. Am. Chem. Soc.*, **91**, 726 (1969).
13) H. Takesada, H. Yamagaki, and A. Wada, *Biopolymers*, **4**, 713 (1966).
14) S. Yamashoji, H. Yoshida, and G. Kajimoto, *Yukagaku*, **25**, 128 (1976).
15) K. Yamaoka and T. Masujima, *Bull. Chem. Soc. Jpn.*, **52**, 1286 (1979).
16) J. C. Leyte, L. H. Zuiderweg, and M. von Reisen, *J. Phys. Chem.*, **72**, 1127 (1968).
17) T. Nozawa and N. Hatano, *Makromol. Chem.*, **141**, 21 (1971).
18) F. P. Cavasino, *J. Phys. Chem.*, **69**, 4380 (1965).
19) K. Tamura, S. Harada, M. Hiraishi, and T. Yasunaga, *Bull. Chem. Soc. Jpn.*, **51**, 2928 (1978).
20) K. Tamura, S. Harada, Y. Funaki, and T. Yasunaga, *Bull. Chem. Soc. Jpn.*, **55**, 813 (1983).
21) L-Aspartyl-L-alanyl-L-histidine *N*-methylamide.
22) A. Tanaka, H. Ogawa, and M. Kamada, *Bull. Chem. Soc. Jpn.*, **36**, 530 (1963).
23) M. Eigen, *Pure Appl. Chem.*, **6**, 97 (1963).
24) T. J. Swift and R. E. Connick, *J. Chem. Phys.*, **37**, 307 (1962).
25) R. G. Wilkins, *J. Chem. Soc.*, **1957**, 4520; **1962**, 4475.
26) M. Eigen and R. G. Wilkins, *Advan. Chem. Ser.*, **49**, 55 (1964).